Eur. Phys. J. E **5**, 471–480 (2001)

THE EUROPEAN PHYSICAL JOURNAL E

EDP Sciences

The DLCA-RLCA transition arising in 2D-aggregation: simulations and mean field theory

A. Moncho-Jordá[1], G. Odriozola[2], F. Martínez-López[1], A. Schmitt[1], and R. Hidalgo-Álvarez[1,a]

[1] Departamento de Física Aplicada, Facultad de Ciencias, Universidad de Granada, Campus de Fuentenueva, 18071 Granada, Spain
[2] Departamento de Química Física y Matemática, Facultad de Química, Universidad de la República, 11800 Montevideo, Uruguay

Received 16 April 2001 and Received in final form 24 May 2001

Abstract. A sticking probability model based on the average cluster lifetime is employed for deducing a kernel capable to describe the kinetics of computer simulated irreversible aggregation processes in two dimensions. The deduced kernel describes not only the time evolution of the cluster size distribution for diffusion limited aggregation (DLCA) and reaction limited aggregation (RLCA) but also for the entire transition region between both regimes. The model predicts a crossover to diffusion limited cluster aggregation for all sticking probabilities at long aggregation times. The time needed for reaching the DLCA limit increases for decreasing sticking probability.

PACS. 82.70.Dd Colloids – 82.40.Np Temporal and spatial patterns in surface reactions – 02.50.-r Probability theory, stochastic processes, and statistics – 82.20.F Stochastic models - chemical kinetics

1 Introduction

Aggregation of colloidal particles occurs in a wide variety of physical, chemical and biological processes [1,2]. Hence, it is of great practical interest to predict the time evolution of the aggregating species from relatively simple theoretical expressions. Smoluchowski's equation has been widely used for this purpose [3,4]. This equation, however, needs a physically deduced aggregation kernel before meaningful conclusions may be drawn from its predictions. So far, diffusion theory combined with concepts of fractal geometry [5], have been the most important tools for describing kinetic and structural aspects of aggregation processes [6,7].

Two limiting aggregation regimes characterized by very different cluster size distributions and cluster fractal dimensions have been reported in literature. For diffusion limited cluster aggregation (DLCA), no repulsive interactions between clusters exist and so, the time spent by a cluster before it reacts with another one is totally controlled by Brownian diffusion. For reaction limited cluster aggregation (RLCA), however, there are strong repulsive interactions that reduce the aggregation rate. If these repulsive interactions correspond to a short range repulsive barrier then the cluster motion is purely Brownian and the aggregates interact only on contact. In this case, the repulsive barrier can be replaced by a sticking probability, P, defined as the fraction of effective collisions that lead to the formation of a new bond [8–10].

The kinetic aspects of the RLCA regime and the DLCA-RLCA transition for repulsive barriers of moderate height have been widely studied in literature [10–15]. Theoretical models capable to describe simulated or experimental data, however, are scarce [16]. Moreover, the complexity of the RLCA regime is enhanced due to the the existence of a crossover to DLCA at very long aggregation times [17,18]. This crossover has been interpreted in terms of spatial cluster density fluctuations which, above a certain aggregation time, t_{cross}, become important [18–22]. Since the Smoluchowski approach does not include these effects, its predictions are not expected to be valid for times longer than t_{cross}.

In this paper, a simple probabilistic model is used for describing the complete DLCA-RLCA transition arising in two-dimensional aggregation [23]. Using Smoluchowski's approach, the proposed model not only reproduces the cluster size distribution obtained from simulations but also predicts the crossover from reaction limited to diffusion limited aggregation at long times in a natural way. This means that the employed aggregation kernel includes the effect of spatial density fluctuations and for that reason, allows the Smoluchowski approach to be used even at very long aggregation times.

The paper is organized as follows: In Section 2, the theoretical background of aggregation kinetics, dynamic

[a] e-mail: rhidalgo@ugr.es

scaling and fractal structure is presented. In Section 3, the probabilistic aggregation model based on the average cluster lifetime is deduced. The computer simulations and numerical methods for solving the Smoluchowski equation are explained in Section 4. In Section 5, simulated data are compared with the theoretical predictions for the DLCA-RLCA transition. Finally, we summarize the results and conclusions in Section 6.

2 Theoretical background

Aggregation may be considered as a non-equilibrium process that consists in the formation of big structures starting from particles and small aggregates [2]. The corresponding coagulation kinetics is usually studied by means of the time evolution of the cluster-size distribution, $n_i(t)$, *i.e.* the number of cluster formed by i constituent particles at time t. Computer simulations [24–26] and experimental results [9,27] have shown that the cluster size distribution reaches a scaling form for large cluster sizes i and long times. This means that $n_i(t)$ may be expressed as $n_i(t) \sim S(t)^{-2}\phi(i/S(t))$ where $S(t) = \sum_i i^2 n_i(t)/\sum_i i n_i(t)$ is the weight average cluster size at time t. This phenomenon, called dynamic scaling, is observed in both, two and three-dimensional coagulation.

Nevertheless, the cluster size distribution alone does not offer a full description of an aggregation process since it does not directly account for the morphology of the aggregates and their spatial distribution. Aggregation of diffusing particles (with or without interactions) gives rise to randomly branched clusters which are usually characterized by a fractal dimension, d_f. The widely accepted values for d_f in two dimensions are 1.45 and 1.55 for DLCA and RLCA, respectively [6,7].

Although the situation is not completely clear in two dimensions, we assume that the average diffusion coefficient for a cluster with a characteristic radius of gyration R_g is given by $D \sim 1/R_g$ [5]. According to fractal theory, the fractal dimension may be assessed using the expression, $R_g \sim i^{1/d_f}$, which relates the radius of gyration to the cluster size i. Consequently,

$$D_i \sim i^{\gamma} \tag{1}$$

where $\gamma = -1/d_f$. Two-dimensional computer simulations using $\gamma < -0.25$ and a size-independent sticking probability, $P = P_0$, lead to a bell-shaped scaling function $\phi(x)$ [25]. In this case, the number average cluster size, $\langle n(t)\rangle$, and the weight average cluster size, $S(t)$, exhibit the same limiting behavior at long aggregation times $\langle n(t)\rangle \sim S(t) \sim t^z$. The scaling exponent, z, depends on the aggregation regime and is related to the size-dependence of the cluster reactivity.

Kinetic and structural aspects are strongly related. On one hand, clusters with a high fractal dimension consist of compact structures with relatively small radii of gyration and hence, large diffusivities. On the other hand, compact structures have a lower cross section and so, collisions with other clusters are less frequent. Both effects exist in mutual competition, the first tends to increase and the second to decrease the aggregation rate.

In order to describe the time dependence of the cluster size distribution, Smoluchowski's equation has been an important theoretical tool for dilute systems [28]. It reads

$$\frac{\mathrm{d}c_i(t)}{\mathrm{d}t} = \frac{1}{2}\sum_{j=1}^{i-1} k_{j,i-j}c_j(t)c_{i-j}(t) - c_i(t)\sum_{j=1}^{\infty} k_{ij}c_j(t). \tag{2}$$

In the case of two dimensions, $c_i(t) = \langle n_i(t)\rangle/A$ represents the average surface concentration of i-size aggregates contained in the system area A. The aggregation kernel, k_{ij}, quantifies the mean rate at which two i and j-size clusters stick and form an $(i+j)$-size cluster. Smoluchowski's approach, however, assumes the time evolution of the reacting system to be a deterministic process since it considers only average values for the aggregate concentrations and neglects fluctuations in the cluster population.

This problem may be avoided using a stochastic master equation approach [29,30]. Therefore, the aggregation state for a reacting system at a fixed time is characterized by a state vector $\mathbf{n} = (n_1, n_2, ..., n_i, ...)$. For irreversible aggregation processes of dilute systems, the time evolution of the probability, $P(\mathbf{n}, t)$, for finding the system in the state $\mathbf{n}$ is given by the master equation

$$\frac{\mathrm{d}P(\mathbf{n},t)}{\mathrm{d}t} = \frac{1}{2A}\sum_{i,j} k_{ij}[(n_i+1)(n_j+1+\delta_{ij})P(\mathbf{n}^*_{ij},t) - n_i(n_j-\delta_{ij})P(\mathbf{n},t)] \tag{3}$$

where δ_{ij} is the well-known Kronecker symbol and $\mathbf{n}^*_{ij}$ is the following displaced state

$$\mathbf{n}^*_{ij} = \begin{cases} (..., n_i+1, ..., n_j+1, ..., n_{i+j}-1, ...) & \text{for } i \neq j \\ (..., n_i+2, ..., n_{2i}-1, ...) & \text{for } i = j. \end{cases}$$

The aggregation kernel, k_{ij}, must be understood as an orientational and morphological average for all clusters. This means also that k_{ij} depends on the cluster shape and particularly, on their fractal dimension. It should be emphasized that the aggregation kinetics is completely determined by the kernel. Most kernels used in the literature are homogeneous functions of i and j. According to van Dongen and Ernst [32], this kind of kernels may be characterized by two exponents, λ and μ, which are defined as

$$\begin{aligned} k_{aiaj} &= a^{\lambda}k_{ij} \qquad i,j \gg 1 \\ k_{ij} &\sim i^{\mu}j^{\lambda-\mu} \qquad j \gg i \end{aligned} \tag{4}$$

where a is a large positive constant. For $\lambda < 1$, the exponents z and λ are related by $z = 1/(1-\lambda)$.

When clusters stick at the first collision ($P = 1$), the aggregation rate is completely determined by the Brownian diffusion of the aggregates (DLCA). For this regime, an explicit expression for the kernel may be

obtained by estimating the rate of collisions for sufficiently long times. In a d-dimensional space, this reasoning yields [6,26]

$$k_{ij}^{Br} \sim (D_i + D_j)(R_i + R_j)^{d-2} \tag{5}$$

where D_i and R_i are the diffusion coefficient and the radius of gyration of an i-size aggregate, respectively. Using equation (1) and taking into account the fractal cluster structure, one finally obtains for $d = 2$:

$$k_{ij}^{Br} = \frac{k_{11}^{Br}}{2}\left(i^{-1/d_f} + j^{-1/d_f}\right). \tag{6}$$

This kernel is homogeneous, having $\lambda = \mu = -1/d_f = -1/1.45 \approx -0.69$.

3 A kernel for the DLCA-RLCA transition

When repulsive inter-particle forces are present, the aggregation rate decreases since only a fraction of cluster-cluster collisions leads to coagulation. If the repulsive potential barrier is of short range, the barrier can be replaced by an effective sticking probability, P. Hence, the clusters movement will still be Brownian. In the limit $P \to 0$, the aggregation process is completely controlled by the cluster reactivity (RLCA). For intermediate values, a continuous transition from DLCA to RLCA is expected. Recently, Odriozola *et al.* presented a probabilistic aggregation kernel for the DLCA-RLCA transition in three dimensions [23]. In this section, we adapt their expression for two dimensional aggregation and explain the necessary steps for deducing it in detail.

In two dimensions, the Brownian kernel may be written as $k_{ij}^{Br} = A/t_{ij}^{dif}$, where A is the surface area of the system and t_{ij}^{dif} represents the average time spent by two freely diffusing i and j-size clusters before they collide.

For a sticking probability lower than unity, the clusters have to collide more than once in order to aggregate. Therefore, the average time, $\langle t\rangle_{ij}$, spent by a given pair of clusters before coagulation becomes longer due to the effect of non-effective collisions. In this case, the aggregation kernel is given by $k_{ij} = A/\langle t\rangle_{ij}$. In order to deduce an analytical expression for $\langle t\rangle_{ij}$, it is useful to distinguish between cluster-cluster collision and cluster-cluster encounter. We call *collision* when two clusters touch each other and define *encounter* as a sequence of consecutive collisions between the same pair of clusters [23]. Thus, an encounter begins at first collision and ends when the clusters aggregate or one of them diffuses away to collide with another cluster. It is convenient to define t_{ij}^{c} as the average time spent by a pair of colliding clusters between two consecutive collisions. Please note that, the average time between two consecutive encounters is already given by t_{ij}^{dif}.

Since P is the sticking probability, $(1 - P)$ gives the probability for a non-effective collision to occur. Let's suppose that two i and j-size clusters coagulate at first contact. This event has a probability P and the time needed for it is t_{ij}^{dif}. If the clusters do not stick, they have two different possibilities, to collide again or to diffuse away. Hence, it is convenient to define P_{ij}^{c} as the probability for the clusters to collide again. Evidently, $(1 - P_{ij}^{c})$ is the probability for the clusters to end an encounter and to diffuse away. Since the cluster cross section grows with cluster-size, it is obvious that the probability P_{ij}^{c} must increase with i and j.

As an example for a more complex situation, the following event is considered: "Two clusters with particular sizes i and j diffuse and collide four times. Then one of them diffuses away and collides two times with a third cluster before it forms a stable bond". The average time for this event consisting of two encounters with four and two collisions, respectively, is given by $t^{ev} = 2t^{dif} + 4t^{c}$. The probability for this event is $P^{ev} = (P^{c})^4(1-P^{c})(1-P)^5P$. Here, the i and j dependence is omitted for the sake of simplicity. In order to determine the average aggregation time $\langle t\rangle$, all possible events weighted by their corresponding probabilities have to be considered. Hence, $\langle t\rangle$ is given by

$$\langle t\rangle = \sum_{ev} q^{ev} t^{ev} P^{ev} \tag{7}$$

where q^{ev} is the number of equivalent events, *i.e.* the number of different events which contribute to the sum with the same average time and probability. This relationship is consistent only if $\sum_{ev} q^{ev}P^{ev} = 1$ is verified.

In order to evaluate equation (7), it is necessary to find a general expression for P^{ev}, t^{ev} and q^{ev}. For this purpose, we evaluated these parameters for all possible events. Table 1 resumes the results for events consisting of less than five collisions. Here, the events are characterized as a sequence of encounters consisting of different number of collisions. For example, $e(m)e(n)$ refers to an event composed by two encounters of m and n collisions, respectively. From Table 1 the following generalized expressions may be deduced

$$\begin{aligned} q^{ev}(k,l) &= \binom{k-1}{l} \\ t^{ev}(k,l) &= (k-l)t^{dif} + lt^{c} \\ P^{ev}(k,l) &= P(1-P)^{k-1}(P^{c})^{l}(1-P^{c})^{k-l-1} \end{aligned} \tag{8}$$

where k stands for the total number of collisions and l for the total number of pairs of consecutive collisions contained in all encounters of a given event. Using these results in equation (7), leads finally to

$$\begin{aligned} \langle t\rangle = \sum_{k=1}^{\infty}\sum_{l=0}^{k-1} \binom{k-1}{l} \left[(k-l)t^{dif} + lt^{c}\right] \\ \times P(1-P)^{k-1}(P^{c})^{l}(1-P^{c})^{k-l-1}. \end{aligned} \tag{9}$$

Here, the limits of the sums are established in order to account for all possible events. Before evaluating equation (9), the normalization condition,

$$\begin{aligned} 1 = \sum_{ev} q^{ev}P^{ev} = \sum_{k=1}^{\infty}\sum_{l=0}^{k-1} \binom{k-1}{l} P(1-P)^{k-1} \\ \times (P^{c})^{l}(1-P^{c})^{k-l-1} \end{aligned} \tag{10}$$

Table 1. Time and probability scheme for events composed by less than five collisions. Here, $e(m)e(n)$ refers to an event composed by two encounters of m and n collisions, respectively. q is the number of equivalent events, k is the number of collisions and l is the number of collision times, t_c.

event	time	probability	q	k	l
e(1)	t_{dif}	P	1	1	0
e(1)e(1)	$2t_{dif}$	$P(1-P)(1-P_c)$	1	2	0
e(2)	$t_{dif}+t_c$	$P(1-P)P_c$	1	2	1
e(1)e(1)e(1)	$3t_{dif}$	$P(1-P)^2(1-P_c)^2$	1	3	0
e(1)e(2) e(2)e(1)	$2t_{dif}+t_c$	$P(1-P)^2P_c(1-P_c)$	2	3	1
e(3)	$t_{dif}+2t_c$	$P(1-P)^2P_c^2$	1	3	2
e(1)e(1)e(1)e(1)	$4t_{dif}$	$P(1-P)^3(1-P_c)^3$	1	4	0
e(1)e(1)e(2) e(1)e(2)e(1) e(2)e(1)e(1)	$3t_{dif}+t_c$	$P(1-P)^3P_c(1-P_c)^2$	3	4	1
e(2)e(2) e(1)e(3) e(3)e(1)	$2t_{dif}+2t_c$	$P(1-P)^3P_c^2(1-P_c)$	3	4	2
e(4)	$t_{dif}+3t_c$	$P(1-P)^3P_c^3$	1	4	3

must be verified. Considering that $\sum_{x=0}^{X}\binom{X}{x}a^x b^{X-x} = (a+b)^X$, equation (10) reduces to

$$1 = \sum_{k=1}^{\infty} P(1-P)^{k-1}\left\{P^c + (1-P^c)\right\}^{k-1} = \sum_{k=1}^{\infty} P(1-P)^{k-1} = P\frac{1}{1-(1-P)} \tag{11}$$

and so, it is correct.

Now, equation (9) can be rewritten as

$$\langle t\rangle = \sum_{k=0}^{\infty}(k+1)t^{dif}P(1-P)^k \times \sum_{l=0}^{k}\binom{k}{l}(P^c)^l(1-P^c)^{k-l} + \sum_{k=0}^{\infty}(t^c - t^{dif})P(1-P)^k \times \sum_{l=0}^{k} l\binom{k}{l}(P^c)^l(1-P^c)^{k-l} \tag{12}$$

where the sum limits were conveniently changed. Taking into account that $\sum_{x=0}^{X}\binom{X}{x}a^x b^{X-x} = (a+b)^X$ and $\sum_{x=0}^{X} x\binom{X}{x}a^x b^{X-x} = Xa(a+b)^{X-1}$, one obtains

$$\langle t\rangle = P\left\{t^{dif}\sum_{k=0}^{\infty}(k+1)(1-P)^k + (t^c - t^{dif})\sum_{k=0}^{\infty}k(1-P)^k P^c\right\} \tag{13}$$

which yields finally

$$\langle t\rangle_{ij} = \frac{1}{P}\left\{t_{ij}^{dif} + (t_{ij}^c - t_{ij}^{dif})(1-P)P_{ij}^c\right\} \tag{14}$$

where we have explicitly indicated the i and j dependence for the different parameters.

Equation (14) express the average time, spent by a pair of cluster before aggregation, as a function of the quantities P, P_{ij}^c, t_{ij}^{dif} and t_{ij}^c. Its reciprocal value is proportional to the irreversible aggregation kernel. This equation predicts average times larger than t_{ij}^{dif} for all sticking probabilities smaller than unity, which means that no-DLCA aggregation rates are always smaller than the corresponding

DLCA rate constants. Defining $\alpha_{ij} = t_{ij}^c/t_{ij}^{dif}$ one finally obtains the following expression for the kernel

$$\begin{aligned} k_{ij} &= \frac{A}{\langle t\rangle_{ij}} \\ &= \frac{A}{t_{ij}^{dif}} \frac{P}{1+(\alpha_{ij}-1)(1-P)P_{ij}^c} \\ &= \frac{k_{ij}^{Br} P}{1+(\alpha_{ij}-1)(1-P)P_{ij}^c}\cdot \end{aligned} \tag{15}$$

This kernel contains the Brownian kernel as limiting case for $P = 1$. For $P \to 0$, the RLCA regime is found. Intermediate values of P reproduce the whole transition region from DLCA to RLCA. According to their definition, t_{ij}^{dif}, P_{ij}^c and α_{ij} are symmetrical functions of the cluster sizes i and j. Hence, the deduced transition kernel is, as expected, also symmetric in i and j.

For further calculations, it is convenient to express the probability P_{ij}^c in terms of the average number of collisions per encounter for a non-aggregating system, $\mathcal{N}_{ij}$. This magnitude may be calculated considering that the probability for a pair of non aggregating clusters ($P = 0$) to perform an encounter consisting of exactly n consecutive collisions is given by $(P_{ij}^c)^{(n-1)}(1-P_{ij}^c)$. Consequently, $\mathcal{N}_{ij}$ may be calculated as

$$\mathcal{N}_{ij} = (1-P_{ij}^c)\sum_{n=1}^{\infty} n(P_{ij}^c)^{(n-1)} = \frac{1}{1-P_{ij}^c}\cdot \tag{16}$$

Unfortunately, an analytical expression for $\mathcal{N}_{ij}$ could not be deduced from theoretical considerations. For further calculations, however, a hypothesis about its size dependency becomes necessary. As mentioned above, $\mathcal{N}_{ij}$ is a symmetrical function of i and j. Moreover, it must be an increasing function of i and j. According to these two restrictions, we propose the simple form $\mathcal{N}_{ij} = \mathcal{N}_{11}(ij)^b$, where $\mathcal{N}_{11}$ is the mean number of collisions between monomers in a non-aggregating system and $b > 0$ is a constant. It should be pointed out that b neither depends on the cluster size nor on the sticking probability, P. Furthermore, it is reasonable to assume that, for diluted systems, the average time between consecutive collisions is very small in comparison with the diffusion time and so, α_{ij} may be neglected in equation (15). With these assumptions, the transition kernel reads finally

$$k_{ij} = \frac{k_{ij}^{Br} P\mathcal{N}_{11}(ij)^b}{P\mathcal{N}_{11}(ij)^b + (1-P)}\cdot \tag{17}$$

This kernel depends on the DLCA dimer formation rate constant, k_{11}^{Br}, the cluster fractal dimension, d_f, the average number of monomer-monomer collision per encounter for a non-aggregating system, $\mathcal{N}_{11}$, the sticking probability, P, and the exponent b. These parameters may be obtained in the following way: k_{11}^{Br} can be determined by fitting the kinetics of DLCA simulations, *i.e.* for $P = 1$. Its value is the same for all other sticking probabilities $P < 1$. The cluster fractal dimension is calculated directly from the structure of the simulated clusters by means of the well-known radius of gyration method. $\mathcal{N}_{11}$ is assessed by averaging the number of collisions per encounter in simulations of non-aggregating monomeric particles. Since P is an input value for the simulations, only the exponent b remains as an unknown global parameter for all sticking probabilities.

It should be pointed out that the deduced transition kernel predicts a crossover to diffusion-limited aggregation for all aggregation processes with a sticking probability smaller than unity. This may be seen by considering that $P\mathcal{N}_{11}(ij)^b \gg (1-P)$ for large clusters. Hence, the second term is negligible in the denominator of equation (17) and so, $k_{ij} \approx k_{ij}^{Br}$. This means that, even for very small sticking probabilities, the final stage of aggregation is always diffusion controlled. However, the time when the crossover occurs increases with decreasing sticking probability.

4 Simulations and numerical computations

Off-lattice simulations of two-dimensional irreversible aggregation processes were performed using periodic boundary conditions. The considered sticking probabilities were $P = 1$, 0.5, 0.1, 0.05, 0.01, 0.005 and 0.001. The simulations were carried out by placing $N_0 = 30\,000$ particles of radius, a, randomly inside a two-dimensional square box avoiding particle overlap. The side length of the square box was set to $L = 9708a$ in order to achieve a surface fraction of 0.001. The monomeric particles were always moved a fixed step-length $l_0 = 0.5a$ in a random direction. Clusters formed by $i > 1$ particles are moved the same distance in a random direction with a probability given by their diffusion coefficient (Eq. (1)) [25]. Since the cluster diffusivity depends on the cluster fractal dimension, a self-consistent method had to be used. For this purpose, several simulation runs were performed until the cluster fractal dimension used in equation (1) matched the one obtained from the structure of the simulated clusters. The fractal dimensions for the considered sticking probabilities from $P = 1$ to 0.001 were determined to be $d_f = 1.45$, 1.46, 1.49, 1.50, 1.53, 1.54 and 1.55, respectively. Rotational cluster motion was not considered. After each translation step, the time is incremented by $\Delta t = 1/(N_C D_{\max})$ whether the cluster is actually moved or not. Here, $N_C(t)$ and $D_{\max}(t)$ are the number of clusters and the largest diffusion coefficient in the whole system at time t, respectively.

A collision is considered to occur when a moved aggregate overlaps with another one. For DLCA, every collision produces aggregation. For non-DLCA, only a fraction given by the sticking probability, P, leads to the formation of a new bond. In order to avoid particle overlap, the position of the moved cluster is always corrected backwards so that only the cluster surfaces are in contact. When aggregation occurs, both aggregates are considered as a new larger cluster that will continue its movement in the following time step. Otherwise, the moved cluster is reflected until it covers the complete step-length, l_0.

The simulations were stopped when less than 100 clusters were left in the system. The simulation time-step was

converted into real time considering a monomer radius of $a = 2.75 \times 10^{-7}$ m and assuming Stokes's law for the monomer diffusivity in water at 298 K.

$$\Delta t_{\mathrm{real}} = \frac{{l_0}^2}{4D} \Delta t_{\mathrm{sim}}. \tag{18}$$

$\mathcal{N}_{11}$ was obtained from simulations with $P = 0$ since it is defined as the mean number of monomer-monomer collisions per encounter in a non-aggregating system.

The time evolution of the cluster-size distribution of the simulated data was compared with the corresponding stochastic solution of the master equation (Eq. (3)) using the deduced transition kernel (Eq. (17)) [29,30] together with the fractal dimensions obtained from the simulations. Furthermore, the same surface fraction and monomeric initial conditions as for the computer simulations were established. The number of initial particles was set to $N_0 = 10^5$ in order to achieve reliable statistics at large aggregation times.

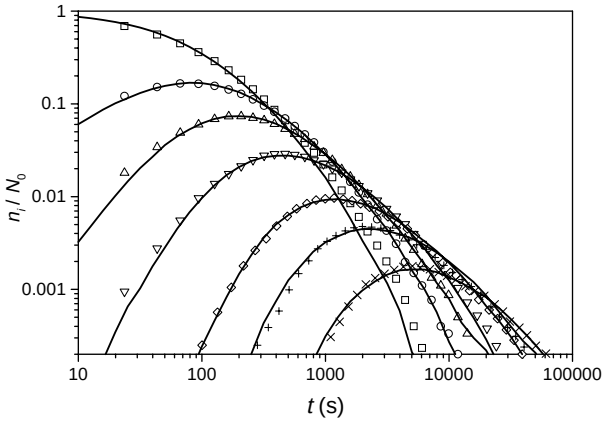

Fig. 1. Time evolution of the normalized cluster-size distribution for $P = 1$. The points correspond to the computer simulated data for monomers up to 25-mers grouped in logarithmically spaced intervals: (□) monomers, (○) dimers, (△) 3-mers, (▽) 4 to 6-mers, (◇) 7 to 10-mers, (+) 11 to 15-mers and (×) 16 to 25-mers. The solid lines represent the corresponding stochastic solution for the Brownian kernel.

5 Results and discussion

Before studying non purely diffusion controlled aggregation processes, we first checked whether the two-dimensional Brownian kernel (Eq. (5)) is capable to correctly describe the time evolution of the cluster-size distribution arising in pure DLCA. For this purpose, dilute systems of sticky particles were simulated ($P = 1$). In this case, the obtained cluster fractal dimension was $d_f = 1.45$. Figure 1 shows that the time evolution of the simulated cluster size distribution is in good agreement with the theoretical prediction calculated from equation (3). From the best fit, the Brownian dimer formation rate constant was obtained to be $k_{11}^{Br} = 4.5 \times 10^{-12}$ m^2/s. This value was also used for fitting the kinetics of processes with sticking probabilities smaller than unity.

In order to check the validity of the deduced transition kernel (Eq. (17)), irreversible aggregation processes in two dimensions were simulated for the sticking probabilities $P = 0.5$, 0.1, 0.05, 0.01, 0.005 and 0.001. The obtained cluster-size distributions for $P = 0.1$, 0.01 and 0.001 are shown as data points in Figure 2. As can be seen, the monomer concentrations decrease monotonously for all sticking probabilities since they only can disappear as they form larger aggregates. Clusters other than monomers must first be generated before they may react and so, the corresponding curves exhibit a clear maximum. As expected, the aggregation processes become slower for decreasing sticking probability.

The simulated data may now be fitted by the corresponding stochastic solutions of Smoluchowski's equation using the proposed 2D transition kernel. Before doing so, it was necessary to determine a reliable value for the still unknown parameter $\mathcal{N}_{11}$. For this purpose, additional simulation runs for $P = 0$ were carried out under the same simulation conditions as used before, and $\mathcal{N}_{11}$ was calculated as the average number of monomer-monomer collisions per encounter. The obtained result was $\mathcal{N}_{11} = 16.1$. Hence, only b remains as a global fitting parameter for all sticking probabilities. The best fit for the complete set of simulated data was obtained for $b = 0.37$. The corresponding stochastic solutions for the time evolution of the cluster-size distribution are included as continuous curves in Figure 2. In all cases, an excellent agreement between the fitted curves and the simulated data is observed. This means that the deduced kernel is capable to reproduce the aggregation kinetics not only for the limiting DLCA and RLCA regimes but also for the complete transition region between them. It should be pointed out that the fitted value of $b = 0.37$ is very close to the value of $b = 0.35$ that we found for three-dimensional aggregation [23] and the value of $b = 0.4$ reported by Thorn and Seesselberg [31]. This indicates that the exponent b seems to be independent on the dimension of space where the aggregation processes occur.

The quality of the fits may also be corroborated by plotting the weight average cluster size as a function of time. As can be seen in Figure 3, the theoretical and simulated curves agree almost perfectly for the different sticking probabilities. Moreover, three different regions may be distinguished. At early stages, the cluster size distribution is still affected by the monomeric initial conditions and the overall cluster growth rate is slow. The time spent in this region is longer the smaller the sticking probability, P, becomes.

After some time, $t > t_{\mathrm{scal}}$, the weight average cluster size shows a power law dependence, $S(t) \sim t^z$. Here, the value of the scaling exponent z increases for decreasing P and reaches a maximum in the RLCA limit. It can be shown that, in this region, the cluster-size distributions become independent of the initial conditions and exhibit dynamic scaling, *i.e.* they may be expressed in terms of a single master curve.

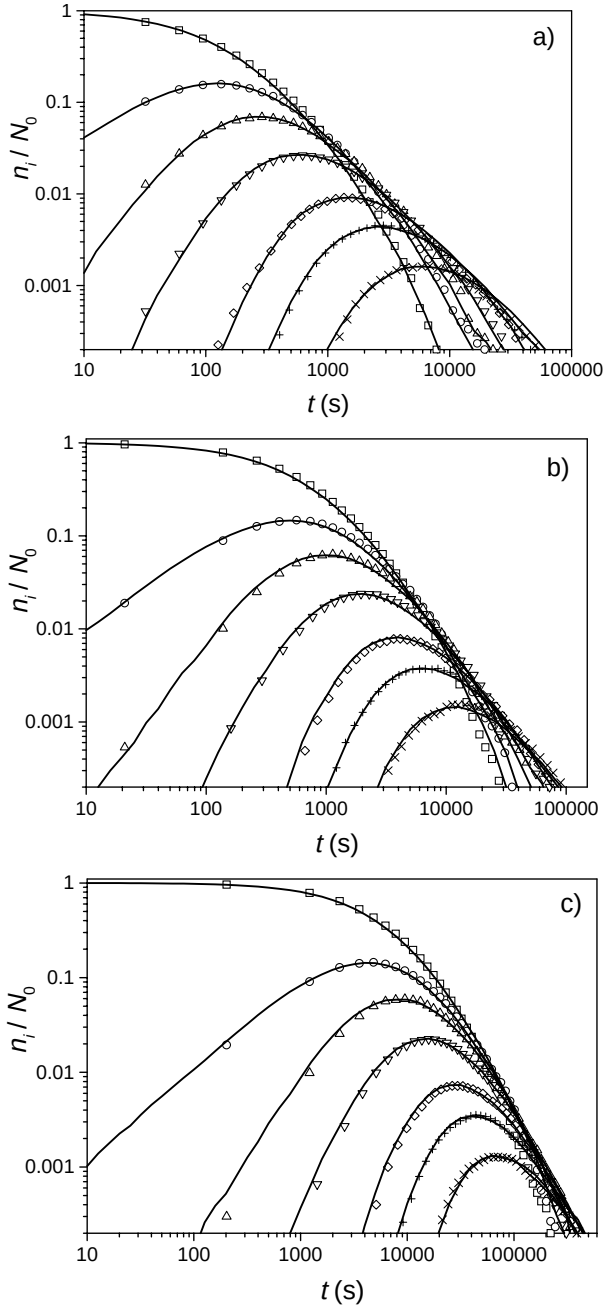

Fig. 2. Time evolution of the normalized cluster-size distribution for the sticking probabilities a) 0.1 b) 0.01 and c) 0.001. The points correspond to the computer simulated data for monomers up to 25-mers grouped in logarithmically spaced intervals: (□) monomers, (○) dimers, (△) 3-mers, (▽) 4 to 6-mers, (◇) 7 to 10-mers, (+) 11 to 15-mers and (×) 16 to 25-mers. The solid lines represent the corresponding stochastic solution for the transition kernel.

At longer aggregation times, the growth rates tend to decrease for all sticking probabilities smaller than unity and the slope of the curves become similar to the one given by the curve for $P = 1$. This phenomenon occurs at a time $t > t_{\rm cross}$ and is known as crossover to Brownian coagulation. As was explained in the theory section, the aggregation rate constants become similar to the Brownian rate

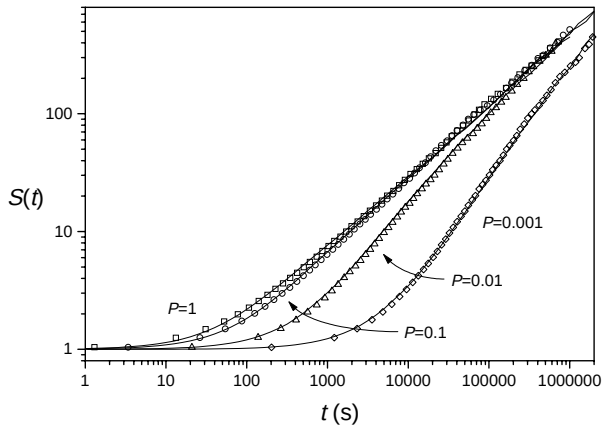

Fig. 3. Time evolution of the weight average cluster-size, $S(t)$, for the sticking probabilities $P = 1$, 0.1, 0.01 and 0.001. The points correspond to the computer simulated data. The solid lines represent the corresponding stochastic solution for the transition kernel.

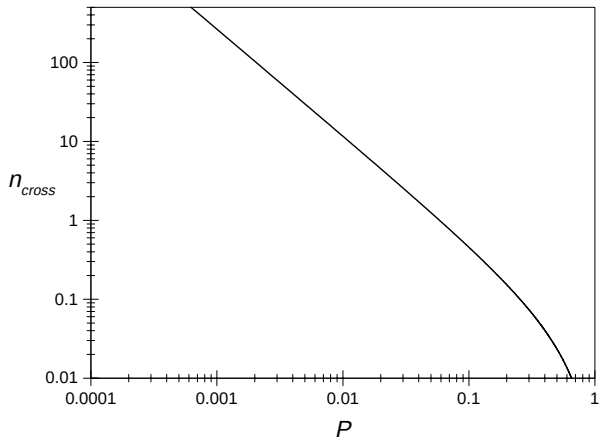

Fig. 4. Critical number average cluster size as a function of the sticking probability.

constants for $P\mathcal{N}_{11}(ij)^b \gg (1-P)$. Using this relationship, a critical cluster size, $n_{\rm cross}$, at which the crossover occurs may be determined considering $i \approx j \approx n_{\rm cross}$. Hence,

$$n_{\rm cross} = \left(\frac{1-P}{P\mathcal{N}_{11}}\right)^{1/2b} . \qquad (19)$$

Figure 4 shows the critical number average cluster size as a function of the sticking probability. As can be seen, $n_{\rm cross}$ increases for decreasing P. This implies that also the time, $t_{\rm cross}$, at which the crossover occurs should be larger for smaller sticking probabilities. In order to check this point, the number average cluster size has been calculated from simulations for different sticking probabilities and plotted *versus* time in Figure 5. For all curves with P smaller than unity, the critical cluster sizes, $n_{\rm cross}$, were obtained using equation (19) and indicated in the plot as horizontal lines. As expected, the corresponding aggregation times increase for decreasing sticking

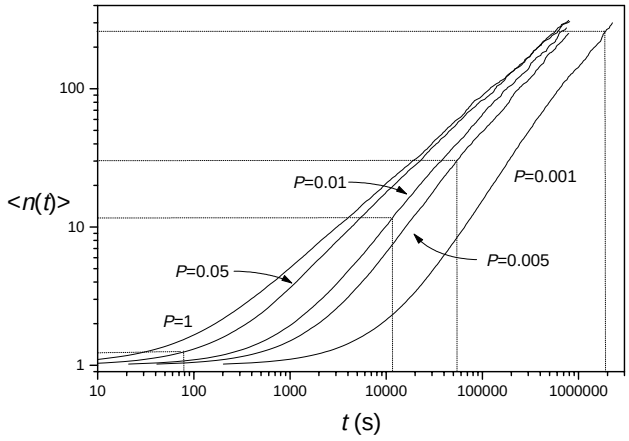

Fig. 5. Time evolution of the number average cluster-size, $\langle n(t)\rangle$, obtained from computer simulations for the sticking probabilities $P = 1$, 0.05, 0.01, 0.005 and 0.001. The critical cluster size obtained from equation (19) and the corresponding crossover times are indicated as horizontal and vertical lines, respectively.

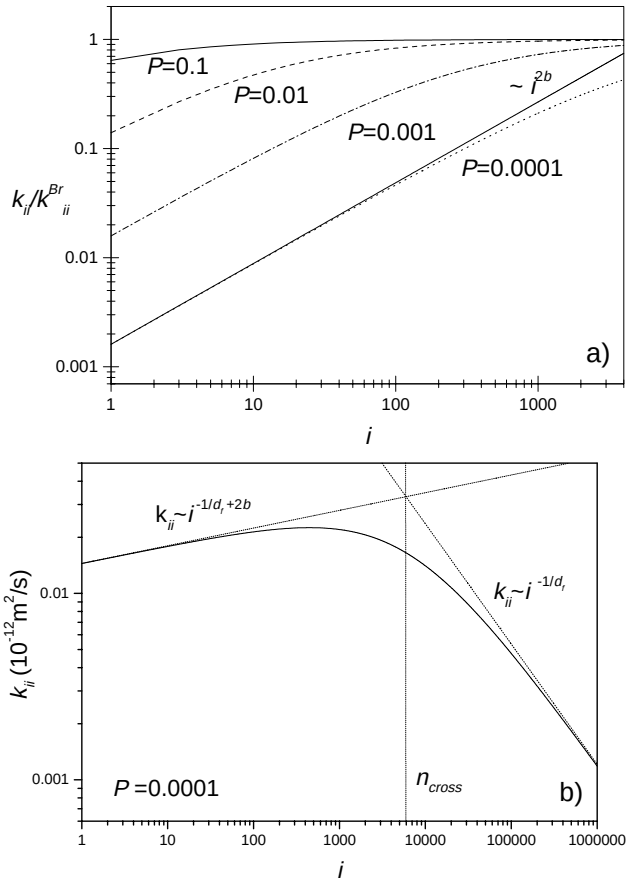

Fig. 6. a) Size dependence of the normalized diagonal elements of the transition kernel, k_{ii}/k_{ii}^{Br}, for $P = 0.1$, 0.01, 0.001, and 0.0001. As indicated in the plot, a power law dependence $k_{ii}/k_{ii}^{Br} \sim i^{2b}$ is observed for low sticking probabilities and small cluster-sizes. b) Size dependence of the diagonal elements of the transition kernel, k_{ii}, for $P = 0.0001$. Two asymptotic regions are observed. For small cluster-sizes, k_{ii} grows as i^{-1/d_f+2b} while for large cluster sizes, a decreasing power law dependence $k_{ii} \sim i^{-1/d_f}$ is found. The corresponding crossover size $n_{\rm cross}$, calculated from equation (19), is indicated as vertical line.

probabilities. Moreover, the crossover from the scaling region to Brownian coagulation can be observed at the indicated crossover times for $P \leq 0.01$, *i.e.* the curves start to bend and their slopes tend towards the DLCA limit. For larger sticking probabilities, however, the critical cluster size becomes so small that the crossover occurs already at very early stages of aggregation. In this case, the system is still affected by the monomeric initial conditions and so, the crossover is not clearly observable.

The above mentioned observations may be studied in more detail considering the size-dependence of the transition kernel. For this purpose, the normalized diagonal elements of the transition kernel, k_{ii}/k_{ii}^{Br}, were plotted in Figure 6a as a function of i for different sticking probabilities. For large cluster sizes, all curves approach unity, *i.e.* the Brownian limit which is characterized by the power law dependence, $k_{ii} \sim i^{-1/d_f}$. According to equation (4), this behavior corresponds to $\lambda = -1/d_f$. Furthermore, for very low sticking probabilities, an additional clearly defined power law dependence is found for clusters smaller than $n_{\rm cross}$. This can be seen more clearly in Figure 6b which represents directly the diagonal elements of the transition kernel for the $P = 0.0001$. For small cluster sizes, the size dependence is given by $k_{ii} \sim i^{-1/d_f+2b}$ which corresponds to $\lambda = -1/d_f + 2b$. This results may be summarized as

$$\lambda = \begin{cases} -1/d_f + 2b & i \ll n_{\rm cross} \\ -1/d_f & i \gg n_{\rm cross}. \end{cases} \qquad (20)$$

It should be pointed out that the size range where the small cluster scaling appears increases for decreasing P. This explains why the scaling region for the weight average cluster size (see Fig. 3) is clearly defined only for very small sticking probabilities. Only in this case, the aggregation kernel preserves its initial power law dependence up to relatively large clusters sizes so that the initially monodisperse cluster size distribution has sufficient time to develop the corresponding scaling behavior. For intermediate sticking probabilities, however, $t_{\rm cross}$ becomes similar to $t_{\rm scal}$ and so, the scaling region is already affected by the crossover to Brownian coagulation. This implies that the observed scaling exponents z fall between the limiting values $z = 1/(1+1/d_f-2b)$ and $z = 1/(1+1/d_f)$, corresponding to pure RLCA and DLCA, respectively. This effect is corroborated by the simulated data shown in Figure 3 where one can observe that z decreases continuously as P increases. The λ values reported in literature for experimental and computer simulated data correspond usually to this short time scaling region, *i.e.* they are obtained for $t_{\rm scal} < t < t_{\rm cross}$.

In our particular case, only for the lowest simulated sticking probability, $P = 0.001$, the time interval $t_{\rm scal} < t < t_{\rm cross}$ for small cluster scaling is long enough so that a reliable value for z could be determined. The obtained value was $z = 1.05 \pm 0.02$. For the DLCA limit, an exponent $z = 0.60 \pm 0.01$ was found. Both values are very close to the theoretical prediction of $z = 1/(1+1/d_f-2b) \approx 1.1$ and $z = 1/(1-1/d_f) \approx 0.59$ for RLCA and DLCA, respectively.

The long-time crossover to Brownian coagulation was also reported for three dimensional aggregation and has been explained previously as a direct consequence of local cluster density fluctuations [22]. Smoluchowski's equation is a mean-field approach to coagulation and describes the aggregation kinetics only in terms of the cluster size distribution, $n_i(t)$. As mean-field we refer to the fact that it does not consider two important effects, the different structures of clusters of a given size and spatial density fluctuations at long times. For a system consisting of a sufficiently large number of clusters, the effects produced by the different cluster structures may be implemented by defining the rate constants, k_{ij}, as morphological and orientational averages for all pairs of reacting clusters of size i and j. But how to account for long time spatial fluctuations? It was shown that this type of fluctuations give rise to a crossover to Brownian coagulation for all diffusion-reaction processes occurring in space with a dimension below a critical value [22]. This means that, under these conditions, all aggregation kernels should converge towards the Brownian kernel for large clusters. The proposed transition kernel does so and hence, accounts for large time cluster density fluctuations in a natural way. Consequently, Smoluchowski's equation remains valid at all times and is capable to describe even the evolution of the cluster size distribution at long times. In other words, the proposed transition kernel may be understood as an *effective* kernel, which considers both effects, cluster structure variations and spatial fluctuations at long times.

6 Conclusions

The kinetics of irreversible aggregation processes arising in two dimensions have been studied using a stochastic master equation approach for solving Smoluchowski's equation. For this purpose, a probabilistic aggregation kernel has been deduced and applied for describing computer simulated data for the DLCA, RLCA and intermediate regimes. The theoretical predictions corresponding to this kernel fit the time evolution of the cluster size distribution for all sticking probabilities, P, with only one global fitting parameter.

For very small sticking probabilities, three different aggregation stages can be distinguished. The cluster-size distribution evolves slowly from its initial monomeric conditions to an intermediate scaling regime characterized by a homogeneity exponent $\lambda = -1/d_f + 2b$. Afterwards, a crossover to Brownian coagulation is observed for all sticking probabilities. In this case, the homogeneity exponent is given by $\lambda = -1/d_f$. The time when the crossover occurs decreases for increasing sticking probability so that the scaling region becomes affected by this effect and finally disappears for sticking probabilities close to unity.

The deduced transition kernel gives a simple explanation for the crossover from RLCA to DLCA observed previously by several authors and explained in terms of spatial cluster density fluctuations. The proposed model predicts that the number of collisions per encounter increases for larger cluster sizes. This implies that two huge clusters are involved in so many collisions per encounter that, even for very low sticking probabilities, they are not able to diffuse away and finally end up forming a stable bond. Hence, a large cluster aggregates almost certainly during its first encounter with another cluster and so, behaves practically as a sticky particle. This means that the deduced transition kernel considers the effect of spatial cluster density fluctuations in a natural way and hence, allows the mean field Smoluchowski approach to be used even at very long aggregation times.

Financial support from "Ministerio de Ciencia y Tecnología, Plan Nacional de Investigación Científica, Desarrollo e Innovación Tecnológica (I+D+I)", MAT 2000-1550-C03-01 is gratefully acknowledged.

References

1. J.K.G. Dhont, *An Introduction to Dynamics of Colloids* (Elsevier, Amsterdam, 1996).
2. R. Hidalgo-Álvarez, A. Martín, A. Fernández, D. Bastos, F. Martínez, F.J. de las Nieves, Adv. Colloid Interface Sci. **67**, 1 (1996).
3. M. von Smoluchowski, Phys. Z. **17**, 557 (1916).
4. M. von Smoluchowski, Z. Phys. Chem. **92**, 129 (1917).
5. T. Vicsek, *Fractal Growth Phenomena* (World Scientific, 1992).
6. R. Jullien, Croat. Chem. Acta **65**, 215 (1992).
7. D.J. Robinson, J.C. Earnshaw, Phys. Rev. A **46**, 2045 (1992).
8. A. Marmur, J. Colloid Interface Sci. **72**, 41 (1979).
9. D.J. Robinson, J.C. Earnshaw, Phys. Rev. A **46**, 2055 (1992).
10. W.D. Brown, R.C. Ball, J. Phys. A **18**, L517 (1985).
11. R. Jullien, M. Kolb, J. Phys. A **17**, L639 (1984).
12. M.Y. Lin, H.M. Lindsay, D.A. Weitz, R.C. Ball, R. Klein, P. Meakin, Phys. Rev. A **41**, 2005 (1990).
13. A. E. González, Phys. Rev. Lett. **71**, 2248 (1993).
14. A. Moncho-Jordá, F. Martínez-López, R. Hidalgo-Álvarez, Physica A **282**, 50 (2000).
15. A. Schmitt, G. Odriozola, A. Moncho-Jordá, J. Callejas-Fernández, R. Martínez-García, R. Hidalgo-Álvarez, Phys. Rev. E **62**, 8335 (2000).
16. R.C. Ball, D.A. Weitz, T.A. Witten, F. Leyvraz, Phys. Rev. Lett. **58**, 274 (1987).
17. F. Family, P. Meakin, T. Vicsek, J. Chem. Phys. **83**, 4144 (1985).

18. K. Kang, S. Redner, P. Meakin, F. Leyvraz, Phys. Rev. A **33**, 1171 (1986).
19. K. Kang, S. Redner, Phys. Rev. A **30**, 2833 (1984).
20. P.G.J. van Dongen, J. Stat. Phys. **53**, 221 (1988).
21. P.G.J. van Dongen, J. Stat. Phys. **54**, 221 (1989).
22. P.G.J. van Dongen, Phys. Rev. Lett. **63**, 1281 (1989).
23. G. Odriozola, A. Moncho-Jordá, A. Schmitt, J. Callejas-Fernández, R. Martínez-García, R. Hidalgo-Álvarez, Europhysics Lett. **53**, 797 (2001).
24. T. Vicsek, F. Family, Phys. Rev. Lett. **52**, 1669 (1984).
25. P. Meakin, T. Vicsek, F. Family, Phys. Rev. Lett. **31**, 564 (1985).
26. P. Meakin, Croat. Chem. Acta **65**, 237 (1992).
27. M.L. Broide, R.J. Cohen, Phys. Rev. Lett. **64**, 2026 (1990).
28. F. Leyvraz, H.R. Tschudi, J. Phys. A **15**, 1951 (1982).
29. D.T. Gillespie, J. Phys. Chem. **81**, 2340 (1977).
30. M. Thorn, M. Seesselberg, Phys. Rev. Lett. **72**, 3622 (1994).
31. M. Thorn, M. Seesselberg, Phys. Rev. Lett. **75**, 3778 (1995).
32. P.G.J. van Dongen, M.H. Ernst, Phys. Rev. Lett. **54**, 1396 (1985).